Built-In Self-Test and Characterization of Polar Transmitter Parameters in the Loop-Back Mode

Jae Woong Jeong and Sule Ozev
Arizona State University
Electrical Engineering
jjeong8@asu.edu, sozev@asu.edu

Shreyas Sen and Vishwanath Natarajan
Intel Corp.
shreyas.sen@intel.com
vishwanath.natarajan@intel.com

Mustapha Slamani
IBM Corp.
slamanim@us.ibm.com

***Abstract*—This paper presents a Built-in self-test (BIST) solution for polar transmitters with low cost. Polar transmitters are desirable for portable devices due to higher power efficiency they provide compared to traditional Cartesian transmitters. However, they generally require iterative test/measurement/calibration cycles. The delay skew between the envelope and phase signals and the finite envelope bandwidth can create intermodulation distortion (IMD) that leads to the violation of the spectral mask and error vector magnitude (EVM) requirements. Typically, these parameters are not directly measured but calibrated through spectral performance analysis using expensive RF equipment, leading to lengthy and costly measurement/calibration cycles. Characterization and calibration of these parameters inside the device would reduce the test time and cost considerably. In this paper, we propose a technique to measure the delay skew and the finite envelope bandwidth, two parameters that can be digitally calibrated, based on the measurement of the output of the receiver in the loop-back mode. Simulation and hardware measurement results show that the proposed technique can characterize the targeted impairments in the polar transmitter accurately.**

I. INTRODUCTION

The advancement of system-on-chip (SoC) technologies has enabled integration of different RF components, such as power amplifier (PA), low-noise amplifier (LNA), and mixer into a single chip. Due to this high level of integration, the test access points are limited to the baseband and RF inputs/outputs of the system. This limited access poses a big challenge particularly for advanced architectures where calibration of internal parameters is necessary and ensure proper operation.

RF polar transmitter architecture is highly adaptable and a promising solution for future wireless communication system in terms of power efficiency. In the polar transmitter, the IQ signal is converted to polar form and divided into an amplitude component and a phase component. The amplitude is used as an envelope to modulate the supply voltage of the PA while the phase modulates the high frequency carrier directly, which leads to a constant amplitude signal. Since the PA's supply voltage is modulated based on the amplitude of the PA output, it saves unnecessary power, thus increasing the efficiency significantly [1].

However, although the polar transmitter has high efficiency, it has inherent disadvantages, namely, differential delay skew between the envelope and phase signals, limited envelope bandwidth, which do not exist in traditional Cartesian transmitters. Additionally, as in the traditional architectures, PA nonlinearity is still a problem this time as nonlinear behavior between baseband control input and RF output. Calibration of delay skew and potentially the envelope bandwidth is essential to ensure operational compliance. At the high level, testing of the polar transmitter is same as testing of Cartesian transmitter. A modulated signal is applied to the input of the transmitter and spectral density at several offset frequencies, EVM, and output power are characterized using vector signal analyzers [2]-[3]. However, such performance-based characterization does not lend to easy calibration as required parameters are not directly measured. Instead, the baseband signal is delayed step-by-step fashion until best performance is found [4].

Recently, an analytical technique has been proposed to measure the internal parameters of polar amplifiers using only RF output signal analysis [5]. This technique, while solving the limited access problem, requires precision RF spectrum analysis, which may or may not be available on a production ATE. The need for such high caliber RF instrumentation is reason why testing RF devices is costly compared to baseband or digital devices. Built-in self-test (BIST) or design-for-test (DFT) solutions that utilize low-frequency analog signals are preferable. Baseband signals can be analyzed with high precision as testers and an even on-chip baseband generally are equipped with higher resolution data converters [6]. Several techniques have been proposed in the literature to reduce the reliance on RF instrumentation. In [7]-[9], simple test signals, such as multi-tone sinusoidal signals, are used for characterization of the transceivers. In [10]-[14], the loop-back configuration is used in order to characterize both the transmitter and the receiver. In [10], [11], the authors derive the analytical model for the entire path and use numerical techniques to solve for transmitter and receiver parameters simultaneously. In [12], similar mathematical models are used in conjunction with specialized signals to achieve an analytical solution.

In this paper, we propose a new BIST solution for the polar transmitter to determine the delay skew and bandwidth limitation using the loop-back configuration. Hence, while RF transmitter parameters are determined, signals are analyzed entirely in baseband, enabling the use of higher resolution digitizers. We use a similar step-by-step approach as in [5], but model the entire loop-back path including the receiver impairments to ensure both accuracy and low cost. Since the loop-back signals differ from the RF signal, we determine specialized test signals to de-embed each parameter of interest. Additionally, our proposed solution enables the measurement

978-3-9815370-2-4/DATE14/©2014 EDAA

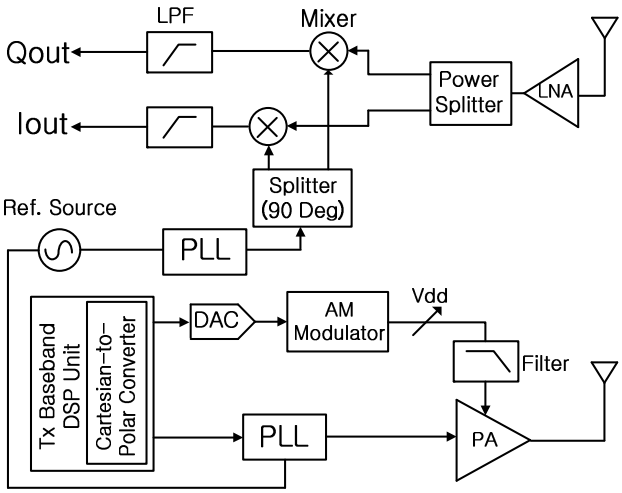

Fig. 1. Transceiver Architecture with Polar Transmitter

and calibration of the impairments inside the device without using external equipment, which leads to improvement of quality and test cost reduction. Experimental results confirm that the delay skew can be measured with sub-ns accuracy and the bandwidth can be determined even with severe limitations.

II. Transceiver with The Polar Transmitter: Advantages and Challenges

Most of the communications systems use variable amplitude signals and the signal amplitude contains part of the information, which necessitates the use of more linear PAs with low efficiency. The discrepancy between the output signal level and the supply voltage, which is dissipated as heat, causes the loss in efficiency. In addition, it leads to poor battery life and increases heat around the PA, thus leads to reliability concerns. As a solution to this problem, the polar transmitter architecture has been proposed. In the polar transmitters, the RF voltage signal (shown in Eqn. (1)) is converted to the polar form as in Eqn. (2). The baseband digital signal processing (DSP) unit calculates the amplitude and the phase of the IQ data as in Eqn. (3).

Fig. 1 shows a typical polar transceiver architecture which consists of polar transmitter and IQ receiver. In the transmitter of Fig. 1, the IQ signal information is converted into a constant amplitude high frequency carrier which is modulated with the phase of the baseband signal, and a low frequency envelope signal which is equal to the magnitude of the original complex IQ signal. The envelope signal is used to modulate the supply of the PA, while the phase modulation is conducted within a phase-locked loop (PLL). The receiver consists of the LNA, mixer, low pass filter, and PLL.

The envelope and phase components of the signal are

$$V_{RF}(t) = I(t)\cdot\cos(\omega_c t) + Q(t)\cdot\sin(\omega_c t) \quad (1)$$

$$V_{RF}(t) = A(t)\cdot\cos(\omega_c t + \phi(t)) \quad (2)$$

$$A(t) = \sqrt{I(t)^2 + Q(t)^2} \quad \phi(t) = \tan^{-1}\left(\frac{Q(t)}{I(t)}\right) \quad (3)$$

divided into two completely different paths and they must arrive at the PA where they are mixed at exactly the same time. However, process variations cause a delay skew between envelope path and phase path, which is damaging to the operation [13]. In addition to the delay skew, there is a low pass filter (LPF) in the envelope path to prevent spectral leakage from the supply modulator [4]. However, this bandwidth (BW) limitation causes distortion of the RF signal at the output of the PA because the envelope signal may have a high BW compared to filter bandwidth. Finally, the response of the PA according to the supply voltage presents nonlinearity, which results in additional distortion. Among these three sources, the delay skew and BW limitation are the most significant contributors and they cause the intermodulation distortion (IMD) to increase. Existing work targeting these parameters requires RF signal analysis at the output of the PA. It is necessary to investigate an alternative method that does not require such high caliber RF instrumentation.

III. Proposed Methodology

One solution for low-cost testing of polar transceiver is to utilize the loop-back mode to achieve a continuous signal path from the baseband input of the transmitter to baseband output of the receiver. The analysis is done at the baseband DSP or the tester using a high resolution ADC (typically 10 bit or higher for ATEs) for on chip analysis. Researchers have used the loop-back configurations for transceivers in order to measure the performance of the system. [10]-[14]. However, no measurement technique in the loop-back mode has been developed for impairments such as the delay skew or bandwidth limitations.

In order to develop a technique to measure the delay skew and envelope bandwidth using the baseband DSP, we first need to configure the transceiver in the loop-back mode. The output of the PA is connected to the input of the low noise amplifier (LNA) through an attenuator. The input of the receiver is down converted to the baseband trough the mixer. The down converted signal is digitized through the ADC and the signal is converted to frequency domain using Fast Fourier Transform. (FFT) Spectral analysis is performed to analyze the IMD.

We need to analyze the effect of the delay skew and limited bandwidth on the system performance. It has been shown in prior work that these two parameters cause IMD [15]. Thus, the simple way to analyze these effect is to use a two-tone signal as the input, as in Eqn. (4) and analyze the output of the receiver in the loop-back mode. The resulting PA output is represented as in Eqn. (5) in polar form where the amplitude signal and the phase signal are given in Eqn. (6). Once the transceiver is configured in the loop-back mode, this signal is down converted to baseband at the receiver output. The amplitude signal and phase information is still maintained after down conversion in frequency domain as in Eqn. (7). A challenge in modeling this system in the loop-back mode is to maintain phase coherence. As Fig. 1 shows, while the two PLLs in the transceiver are synchronized by the same reference source, their phase relation will be random every time a measurement

$$V_{RF}(t)=\frac{1}{2}\left(\cos(\omega_c t-\omega_m t)+\cos(\omega_c t+\omega_m t)\right)=\cos(\omega_m t)\cdot\cos(\omega_c t) \quad (4)$$

$$V_{RF}(t)=\cos(\omega_m t)\cdot\cos(\omega_c t)=a_y(t)\cdot\cos(\omega_c t+\varphi_y(t)) \quad (5)$$

$$a_y(t)=\left|\cos(\omega_m t)\right| \quad \varphi_y(t)=\frac{\pi}{2}\left(1-c(t)\right) \quad (6)$$

$$V_{RX}(t)=G_{RX}\cdot a_y(t)\cdot c(t) \quad (7)$$

$$\begin{aligned} V_{RX\text{ with Delay Skew}}(t) &= 0.5\times G_{RX}\cdot a_y(t)\cdot c(t+\tau) \\ &= \frac{G_{RX}}{2}\left(a_0+\sum_{m=2,4,\cdots,M} a_m\cos(m\omega_m t)\right)\times\left(\sum_{n=1,3,5,\cdots} c_n\cos(n\omega_m(t+\tau))\right) \\ &= \frac{1}{2}G_{RX}\left(a_0+a_2\cos(2\omega_m t)+a_4\cos(4\omega_m t)+\cdots a_M\cos(M\omega_m t)\right) \\ &\times\left(c_1\cos(\omega_m(t+\tau))+c_3\cos(3\omega_m(t+\tau))+\cdots\right) \end{aligned} \quad (8)$$

is taken. Therefore it is necessary to include a random phase offset in the receiver LO signal that changes at every step.

This additional variable prevents us from using any phase-related information. In order to analyze the impact of delay skew and BW limitation in the loop-back mode, we inject a time delay, τ, into the envelope signal and express the envelope signal using a Fourier series. The resulting signal at the output of the receiver can be expressed as in Eqn. (8). Since the envelope has a square waveform, the bandwidth of the signal is infinite. However, it has finite frequency components due to the limited bandwidth of reconstruction filter and the supply modulator. The delay skew between the envelope and the phase signal also causes the IMD levels to increase. In addition, the nonlinearity of the PA adds to the IMD levels. The effects of all of these contributors are intertwined and they are combined in a nonlinear fashion with additional unknowns. Thus, we need to isolate them in the loop-back mode in order to measure these parameters respectively.

A. Isolation of Transceiver Nonlinearity in the Loop-Back Mode

While the PA input has constant amplitude, removing AM/AM and AM/PM distortion effects, the relation between the envelope input and the PA output is nonlinear. This nonlinear relation also causes AM/AM and AM/PM distortion. In the proposed technique, no phase information is used. However, AM/AM distortion due to the nonlinearity of the PA response with respect to the control input, as well as the resulting IMD levels would pose a problem in terms of determining the delay skew. In order to minimize the effect of this nonlinearity during the delay skew measurements, the envelope signal needs to be located within a range where the PA presents the most linear behavior. While this is not necessarily the case for normal mode of operation, our goal here is to suppress the effect of this nonlinearity in order to emphasize the other sources of IMD. However, using the PA in the linear range in terms of its control input poses another challenge for characterization as it may be necessary to include a DC offset in the signal, altering the overall model. (Eqn. (8))

As an example, Fig. 2 shows the output of the receiver versus the PA supply input voltage for the transceiver in the loop-back mode. As seen in the Fig. 2, the gain (and thus the output) follows a nonlinear behavior at very low input levels. If we want to eliminate the distortion due to this nonlinearity, this region at the input should be avoided. In addition to the PA, the receiver needs to operate in linear region to eliminate its contributors to the IMD levels. The amplitude of the input signal at the receiver should be sufficiently small to ensure linear operation. Luckily, if the input of the LNA is limited to 3-6 dB below the 1 dB compression point, the IMD generated by the receiver will be negligible. Therefore an attenuator between transmitter output and receiver input is used to ensure that the receiver operates in the linear region.

B. Isolation of the BW Limitation in the Loop-Back Mode

The envelope signal that is measured at the output of the receiver has a square wave component, which is same as the envelope signal at the PA output. If the envelope signal includes a sufficient number of harmonics, the distortion caused by the limited bandwidth is minimized. In order to enable this, we need to keep M in Eqn. (8) large. At around M>10, the distortion contribution of the BW limitation can be ignored. Although the BW of the envelope path is still unknown, we can obtain large M by applying a sufficiently low-bandwidth baseband signal because the envelope signal can include large number of harmonics with the low-bandwidth.

Once the contributions due to nonlinearity of the transceiver and BW limitations are minimized, the delay skew is the major contributor to IMD and we can calculate it in the loop-back mode analytically. Once this delay skew is determined, it can be compensated digitally, thus minimizing its contribution to IMD, which will lead to the measurement of the envelope BW. Thus our proposed technique consists of the following steps:

- **Step 1:** Configure the transceiver in the loop-back mode
- **Step 2:** Apply a low-bandwidth two-tone signal to the transmitter input, measure baseband third order IMD (IMD3) at the output of receiver, and calculate the delay skew analytically
- **Step 3:** Digitally compensate for the delay skew in the envelope signal
- **Step 4:** Increase the bandwidth of the baseband signal, measure the inter modulation distortion at the output of the receiver output, and calculate M, hence the envelope BW

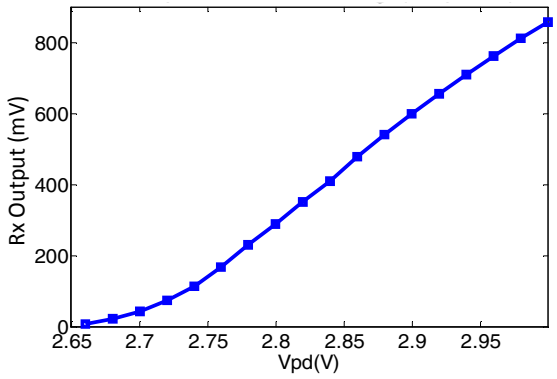

Fig. 2. PA Supply Input Voltage versus Receiver Output

C. *Measurement of Parameters with DC Offset in the Envelope Signal and Attenuation in the Loop-Back Mode*

As mentioned in the previous section, the IMD3 contribution of the PA nonlinearity can be suppressed by operating the PA within a range that presents the most linear behavior with respect to the control voltage. However that necessitates the inclusion of DC offset in the two-tone signal, which would alter the model completely. With the DC voltage, the output of the PA and the receiver can be expressed as in Eqn. (9) and Eqn. (10), respectively. The output amplitude and the DC offset in Eqn. (10) can be obtained as in Eqn. (11).

Note that with the two-tone test, the effect of random phase mismatch between the transmitter and receiver PLL is eliminated from the equations. The effect of this phase offset is a part of the term G'_{RX}, which will be treated as an unknown for each separate step. By using comparative analysis, it can be eliminated from calculation.

The IMD level of k^{th} harmonic (IMD_k) can be calculated from Eqn. (10). The highest power harmonic, which is the third order harmonic, can be calculated using Eqn. (12). Since we will be using spectral analysis at the output, we can coherently measure the magnitude of this distortion component, which is given in Eqn. (12). Note that since $A_{RX,out}$ is also measured, the effect of the unknown gain is eliminated from the IMD3 expression. Hence, the delay skew can be calculated by measuring the IMD3 component since it is the only unknown.

Once we calculate the delay skew, we need to determine the finite envelope bandwidth in the loop-back mode. First the delay skew is compensated and the transceiver still needs to operate in linear-region. Thus, we apply the same DC offset into input baseband signal and set the same attenuation in the attenuator. Then a two-tone input with relatively high frequency can be applied to the input of the polar transmitter.

$$V_{PA,out}(t)=\left(A_{PA,out}\times\left|\cos(\omega_m t)\right|+\Delta V_{PA,out}\right)c(\omega_m t+\tau)\cos(\omega_c t) \tag{9}$$

$$\left(A_{PA,out}=\left(G(v_{dd2})-G(v_{dd1})\right)\times A_{in},\Delta V_{PA,out}=G(v_{dd1})\times A_{in}\right)$$

$$V_{RX}(t)=\frac{1}{2}\left(A_{RX,out}\times\left|\cos(\omega_m t)\right|+\Delta V_{RX,out}\right)c(\omega_m t+\tau) \tag{10}$$

$$\begin{pmatrix} A_{RX,out}=G'_{RX}\times\left(G(v_{dd2})-G(v_{dd1})\right)\times A_{in} \\ \Delta V_{RX,out}=G'_{RX}\times G(v_{dd1})\times A_{in},\quad G'_{RX}=G_{RX}\cos(\varphi_{RF}-\varphi_{LO}) \end{pmatrix} \tag{11}$$

$$\left|IMD_3\right|=0.5\times\sqrt{\left(A_{RX,out}\times a_3\right)^2+\left(A_{RX,out}\times b_3+\Delta V_{RX,out}\times c_3\right)^2} \tag{12}$$

$$\begin{pmatrix} a_3=-\frac{2}{\pi}\left[\frac{1-\cos(4\tau)}{4}+\frac{\cos(2\tau)-1}{2}\right] \\ b_3=-\frac{2}{\pi}\left[\frac{\sin(2\tau)}{2}-\frac{\sin(4\tau)}{4}\right],\quad c_3=\frac{-4}{3\pi} \end{pmatrix} \tag{13}$$

$$M=2\rightarrow\left|IMD_3\right|=\frac{1}{4}\times\left|A_{RX,out}\left[2a_0c_3+a_2(c_1+c_5)\right]+\Delta V_{RX,out}\times c_3\right|$$

$$M=4\rightarrow\left|IMD_3\right|=\frac{1}{4}\times\left|A_{RX,out}\left[2a_0c_3+a_2(c_1+c_5)+a_4(c_3+c_7)\right]\right.$$
$$\left.+\Delta V_{RX,out}\times c_3\right| \tag{14}$$

TABLE I. SIMULATION RESULTS

Parameter	RMS Error	Injection Limit
Delay Skew	0.00053 ns	[0ns, 2ns]
M	0	[1, 5]

The amplitude of the IMD3 with the DC offset voltage at the output of the receiver can be expressed as in Eqn. (14). The direct relation between M and the amplitude of IMD3 at the baseband output of the receiver enables us to generate a lookup table. Thus, once the IMD3 level is measured, the amplitude of IMD3 is compared with the calculated values in the lookup table. From the IMD3 measurement, we can determine the number of frequency components that are included in the passband of the filter. Once the number of frequency components is determined, then the BW of the envelope signal can be estimated since M is directly related to the filter BW. In order to calculate more accurate BW, we need to repeat this measurement several times with different baseband signal frequencies and interpolate the results.

IV. EXPERIMENTAL RESULTS

A. *Simulation Results*

In order to evaluate our new BIST solution for a wide variety of delay/BW scenarios, MATLAB model of the transceiver was implemented in the loop-back mode by adding an attenuator in the TX-RX path with an unknown delay. Monte-Carlo simulations using the MATLAB model were conducted to inject various delay and BW limitation conditions, and our proposed technique in the loop-back mode is used to determine the injected parameters. Table I shows the results of the simulations. These results indicate that the proposed technique accurately determines the desired parameters.

B. *Hardware Measurement Results*

The polar transceiver was emulated using bench equipment and a commercial PA. In addition, a receiver was also constructed using IQ demodulator. The polar transmitter was implemented using the PA module (Hittite Microwave HMC450QS16G), an arbitrary waveform generator (Agilent 33250A), and a vector signal generators (Agilent N5182A). The receiver was implemented using signal analyzer (Agilent

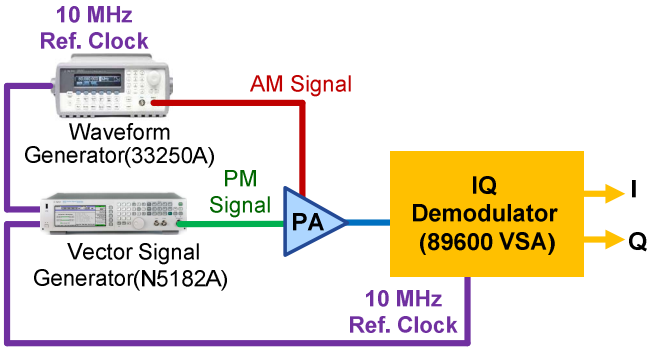

Fig. 3. Clock Synchronization to Ensure Delay Skew Stays Stable during the Course of the Measurement

N9020A), signal demodulation software (Agilent 89600 VSA) and the baseband digital signal processing (DSP) unit was built using MATLAB. The arbitrary waveform generator is used to generate the envelope signal while the vector signal generator is used to generate the phase modulated (PM) signal. Both the envelope and the PM signals should have same clock frequency and be phase locked together in order to extract the delay skew. Fig. 3 shows measurement set-up with clock synchronization. Synchronization between the envelope and phase generators is ensured by locking the clock of these two pieces of equipment. This clock synchronization enables that the delay skew remains constant between the envelope path and the phase path. However, phase coherence is not ensured as it will be the case for an IC implementation. In addition, the reference clock source in the receiver also should be same as one in the polar transmitter. Therefore, as seen in Fig. 3 instruments use same clock source by connecting external 10 MHz output of the vector signal generator to 10 MHz input of the arbitrary waveform generator and 10 MHz input of the vector signal generator to 10 MHz output of the signal analyzer.

For delay skew measurement, the envelope and PM signals of the low BW two-tone signal are applied to the supply and RF input of the PA respectively to implement the polar transmitter. The output of the PA is applied to the input of the IQ demodulator and the output of the IQ demodulator is captured in 89600 VSA software made by Agilent Technologies. Fig. 4 shows the experimental set-up for the polar transceiver. We took FFT of the captured signal using MATLAB. Fig. 5 shows the FFT result of the output of the receiver. Then we can measure the IMD3 to determine the delay skew.

In order to verify the accuracy of the proposed delay skew measurement technique, we use the baseband output in the time domain. The delay skew in the transmitter is measured manually in time domain in order to compare the proposed technique with traditional method. Fig. 6 shows the waveform to determine the delay skew. The delay skew is time difference between A and B in Fig. 6. Table II summarizes the comparison of the results. As these results indicate, the

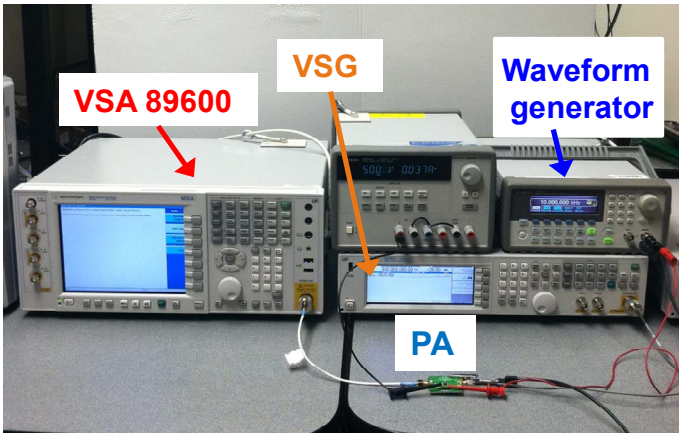

Fig. 4. Measurement Setup

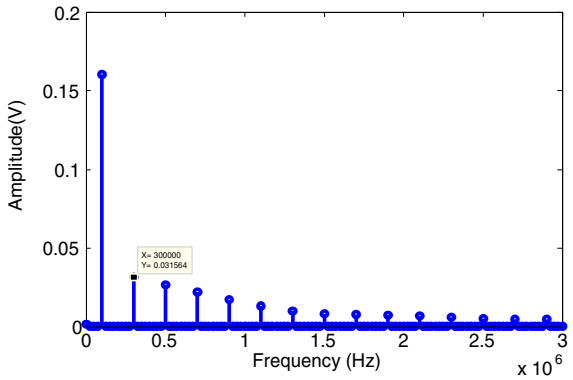

Fig. 5. FFT results of the Output of the Receiver

proposed technique is able to measure the delay skews accurately within ns error. Note that compared to [5], the proposed technique provides better accuracy due to the baseband signal analysis, which can be more accurate than RF signal analysis.

C. *Accuracy of BW Measurement*

Once we calculate and compensate the delay skew in the loop-back mode, we determine the finite bandwidth in the envelope signal by applying the relatively high bandwidth two-tone signal to the input of the transmitter. Since the other effects such as delay skew and nonlinearity of the transceiver are already minimized, the IMD3 at the output of the receiver is mainly due to the finite envelope bandwidth and the offset voltage. We compare the measured amplitude of IMD3 with the calculated values in the lookup table. Table III shows the amplitude of IMD3 according to number of harmonics (M) included in the envelope signal. As seen in Table III, there is only a small error between the measured IMD3 and the calculated values. Based on Table III, by comparing the measured IMD3 with calculated value, the number of the harmonics that are included in the passband of the filter can be determined.

D. *Test Time*

The proposed technique requires three steps. (a) voltage sweep at the PA supply input to determine the linear range (b) measurement of delay skew, and (c) measurement of the envelope BW. In order to increase the resolution of the BW measurement, step (c) needs to be repeated multiple times with varying baseband input frequencies. All of the above mentioned steps require FFT at the output of the receiver. We use a 1024-point FFT. The signal capture time for each step is around 128μs. FFT takes the most time with around 1 ms of computation time. Additional computation time for Eqn. (1)

TABLE II. ACCURACY OF DELAY SKEW MEASUREMENTS WITH THE PROPOSED TECHNIQUE

Case	Measured delay	Calculated delay	Error
1	470 ns	469.51 ns	0.1 %
2	850 ns	849.09 ns	0.1 %
3	1160 ns	1158.81 ns	0.1 %

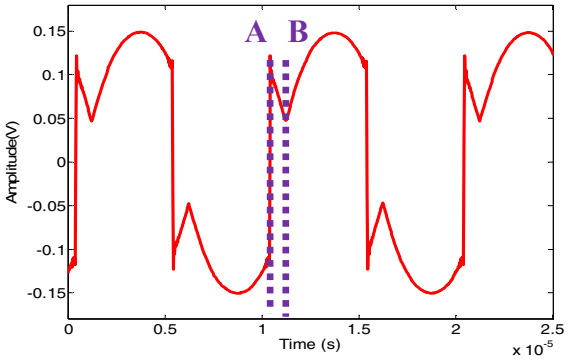

Fig. 6. Measured Output Signal of the Receiver in Time Domain

through Eqn. (15) is negligible. Note that the proposed technique uses same test set-up for all measurement steps. Hence there is no signal source or output switching overhead. Assuming step (c) is repeated 7 times, the overall test time is less than 10 ms.

V. CONCLUSION

In this paper, we propose a new BIST solution to measure the internal calibration parameters for polar transmitter, namely the delay skew between the envelope and phase signals and the finite envelope in the loop-back mode. Previously proposed technique to obtain same parameters requires expensive RF spectrum analyzers which generally do not provide more than 8-bit resolution. In order to solve this problem, we configure the transceiver in the loop-back mode, observe the baseband output of the receiver, and relate the delay skew and BW limitation to the magnitude of the IMD. We devise special test signals in the loop back mode, which leads to isolation of the effect of one parameter at a time. First we calculate the delay skew from the measured IMD3 at the output of the receiver. After compensating for the effect of delay skew, we measure the finite envelope BW. From the second measurement of IMD3 in the loop-back mode, we can estimate the finite envelope bandwidth by comparing the measured IMD3 with a lookup table that consists of the calculated IMD3 values according to the number of harmonics included in the passband of the reconstruction filter. Simulation and hardware measurements show that our proposed BIST solution determines the desired parameters in the loop-back mode accurately.

ACKNOWLEDGEMENT

This work is supported by SRC with contract number 1836-084 and by NSF with contract number 1128566.

TABLE III. COMPARISON OF MEASURED AND CALCULATED VALUES FOR VARIOUS VALUES OF M

M	Measured IMD3	Calculated IMD3
2	0.02 V	0.019 V
4	0.034 V	0.033 V

REFERENCES

[1] B. Kim, J. Moon, and I. Kim, "Efficiently Amplified," *IEEE Microwave Magazine*, vol.11, no.5, pp.87-100, Aug. 2010.

[2] P. Reynaert and M.S.J. Steyaert, "A 1.75-GHz polar modulated CMOS RF power amplifier for GSM-EDGE," *IEEE Journal of Solid-State Circuits,* vol.40, no.12, pp. 2598- 2608, Dec. 2005.

[3] M. Youssef, A. Zolfaghari, B. Mohammadi, H. Darabi, and A.A. Abidi, "A Low-Power GSM/EDGE/WCDMA Polar Transmitter in 65-nm CMOS," *IEEE Journal of Solid-State Circuits,* vol.46, no.12, pp.3061-3074, Dec. 2011.

[4] J. Kitchen, C. Chu, S. Kiaei, and B. Bakkaloglu, "Supply Modulators for RF Polar transmitters," in *IEEE Radio Frequency Integrated Circuit Symposium*, June 2008, pp.417-420.

[5] J.W. Jeong, S. Ozev, S. Sen, and T.M. Mak, "Measurement of envelope/phase path delay skew and envelope path bandwidth in polar transmitters," in *31st IEEE VLSI Test Symposium,* May 2013, pp.1-6.

[6] A. Valdes-Garcia, J. Silva-Martinez, and E. Sanchez-Sinencio, "On-Chip testing technique for RF wireless transceivers," *IEEE Design and Test of Computers,*vol. 23, no.4, pp268-277, Apr. 2006.

[7] D. Lee, R. Senguttuvan, and A. Chatterjee, "Efficient testing of wireless polar transmitters," in *14th IEEE International Mixed-Signals, Sensors, and Systems Test Workshop*, June 2008. pp.1-5.

[8] D. Lee, V. Natarajan, R. Senguttuvan, and A. Chatterjee, "Efficient Low-Cost Testing of Wireless OFDM Polar Transceiver Systems," in *17th Asian Test Symposium,* Nov. 2008, pp.55-60.

[9] A. Haider and A. Chatterjee, "Low-cost alternate EVM test for wireless receiver systems," in *23rd IEEE VLSI Test Symposium,* May 2005, pp. 255- 260.

[10] A. Nassery, O.E. Erol, S. Ozev, and M. Verhelst, "Test Signal Development and Analysis for OFDM Systems RF Front-End Parameter Extraction," *IEEE Transactions on Computer-Aided Design of Integrated Circuits and Systems,*vol.31, no.6, pp.958-967, June 2012.

[11] E.S. Erdogan and S. Ozev, "Detailed Characterization of Transceiver Parameters Through Loop-Back-Based BiST," *IEEE Transactions on Very Large Scale Integration (VLSI) Systems,*vol.18, no.6, pp.901-911, June 2010.

[12] A. Nassery and S. Ozev, "An analytical technique for characterization of transceiver IQ imbalances in the loop-back mode," in *Design, Automation & Test in Europe Conference & Exhibition (DATE),* Mar. 2012, pp.1084-1089.

[13] A. Haider, S. Bhattacharya, G. Srinivasan and A. Chatterjee, "A system-level alternate test approach for specification test of RF transceivers in loopback mode," in *18th International Conference on VLSI Design,* Jan. 2005, pp. 289- 294.

[14] S. Bhattacharya and A. Chatterjee, "A built-in loopback test methodlogy for RF transceiver circuits using embedded sensor circuits," *in Proc. IEEE ATS*, Nov. 2004, pp. 68-73.

[15] F.H. Raab, "Intermodulation distortion in Kahn-technique transmitters," *IEEE Transactions on Microwave Theory and Techniques,*vol.44, no.12, pp.2273-2278, Dec. 1996.

[16] D. Rudolph, "Out-of-band emissions of digital transmissions using Kahn EER technique," *IEEE Transactions on Microwave Theory and Techniques,* vol.50, no.8, pp. 1979- 1983, Aug. 2002.

[17] L. R. Kahn, "Single sideband transmission by envelope elimination and restoration," *Proc. IRE*, vol. 40, pp. 803–806, July 1952.

[18] D. Rudolph, "Kahn EER technique with single-carrier digital modulations," *IEEE Transactions on Microwave Theory and Technique*, vol.51, no.2, pp.548-552, Feb. 2003.